Title: Microwave dielectric properties of low-fired Li_2SnO_3 ceramics co-doped with MgO–LiF

Author: Zhifen Fu Peng Liu Jianli Ma Baochun Guo Xiaoming Chen Huaiwu Zhang

PII: S0025-5408(16)30019-8
DOI: http://dx.doi.org/doi:10.1016/j.materresbull.2016.01.019
Reference: MRB 8611

To appear in: *MRB*

Received date: 22-8-2015
Revised date: 23-12-2015
Accepted date: 10-1-2016

Please cite this article as: Zhifen Fu, Peng Liu, Jianli Ma, Baochun Guo, Xiaoming Chen, Huaiwu Zhang, Microwave dielectric properties of low-fired Li2SnO3 ceramics co-doped with MgOndashLiF, Materials Research Bulletin http://dx.doi.org/10.1016/j.materresbull.2016.01.019

Microwave dielectric properties of low-fired Li_2SnO_3 ceramics co-doped with MgO-LiF

Zhifen Fu[a, b], Peng Liu[a, *], Jianli Ma[b], Baochun Guo[a], Xiaoming Chen[a], Huaiwu Zhang[c]

[a]*College of Physics and Information Technology, Shaanxi Normal University, Xi'an, 710062, China*

[b]*College of Science, Anhui University of Science and Technology, Huainan, 232001, China*

[c]*The Key Laboratory of Electronic Thin Film and Integrated device, University of Electronic Science and Technology of China, Chengdu, 610054, China*

[*] **Corresponding author:** liupeng@snnu.edu.cn (P. Liu)

Graphical Abstract

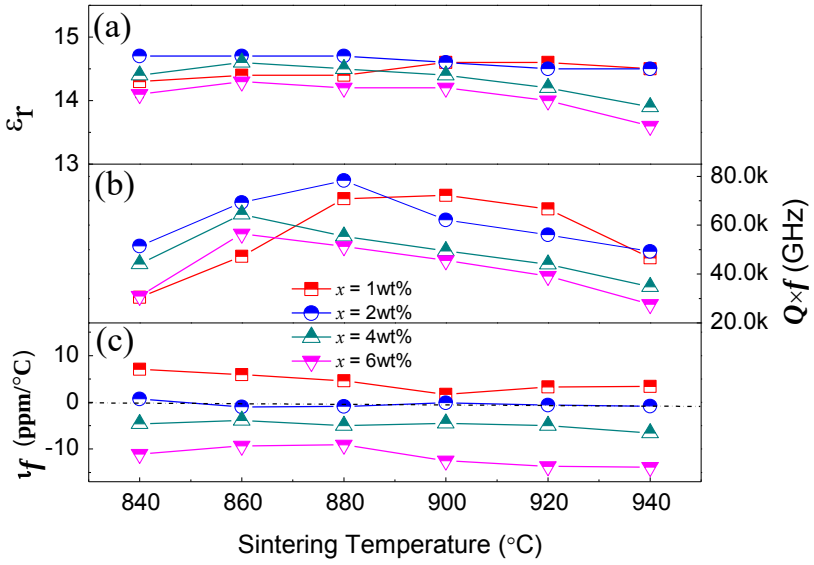

Highlights

- Low-fired Li_2SnO_3 ceramics co-doped with MgO-LiF are fabricated.
- A novel phase $Li_2Mg_3SnO_6$ was observed with increasing MgO content.
- Addition of LiF lowered sintering temperature of Li_2SnO_3-MgO ceramics to 880 °C.
- The microwave dielectric properties of ceramics were optimized by $Li_2Mg_3SnO_6$ phase.
- Ceramics with well dielectric properties are suitable for LTCC applications.

Abstract:

Low-fired Li_2SnO_3 ceramics co-doped with MgO-LiF were fabricated by a conventional solid-state route, and their sinterability, microwave dielectric properties were investigated. With increasing MgO content, a novel phase $Li_2Mg_3SnO_6$ was formed. A near-zero τ_f value was obtained at 1325 °C for Li_2SnO_3-8wt% MgO ceramics. Furthermore, LiF addition not only successfully lowered the sintering temperatures to 880 °C but also promoted formation of $Li_2Mg_3SnO_6$. The microwave dielectric properties of Li_2SnO_3-8wt% MgO ceramics were further optimized with increasing $Li_2Mg_3SnO_6$ content. The excellent microwave dielectric properties (ε_r = 14.7, $Q \times f$ = 78400 GHz, and τ_f = -0.9 ppm/°C) were achieved at 880 °C for Li_2SnO_3-8wt% MgO-2wt% LiF ceramics, which is compatible with Ag electrodes and suitable for the low-temperature co-fired ceramics (LTCC) applications.

Keywords: A. Ceramics; A. Oxide; B. Microstructure; C. X-ray diffraction; D. Dielectric properties

1. Introduction

With developing wireless and mobile communication industry, microwave dielectric ceramics have been widely used in fields such as telecommunication, radar and navigation. Nowadays, the low-temperature co-fired ceramic (LTCC) multilayer devices are very attractive subjects due to their alternating compact of dielectric ceramic substrates and internal metallic electrode layers. Four characteristic properties are required for LTCC applications [1]: appropriate dielectric constant ($\varepsilon_r \leq 25$) to avoid signal delay, high quality factor ($Q \times f \geq 5000$ GHz) for selectivity, a near-zero temperature coefficient of resonant frequency ($|\tau_f| \leq 10$ ppm/°C) for stability, lower sintering temperature (Ts < 960 °C) and excellent chemical compatibility with the Ag electrode. Several methods have been developed for this purpose: using ultrafine nanopowders as raw materials [2], searching for new ideal low-temperature sintered ceramic material [3], or adding sintering aids into dielectric ceramic systems [4]. Among them, adding sintering aids is the most effective and cheapest method to improve the sinterability of ceramics.

Recently, lithium based oxide ceramics Li_2MO_3 (M = Sn, Ti, Zr), Li_3MO_4 (M = Sb, Ta), and $Li_2ATi_3O_8$ (A = Mg, Zn) have aroused considerable attention from materials research and engineering applications [5~7]. Among them, Li_2TiO_3 ceramic with rock salt structure received special attention due to its good dielectric properties: $\varepsilon_r \sim 19$, $Q \times f$ above 23600 GHz, and $\tau_f = 38$ ppm/°C [5]. However, its Ts (around 1200 °C) are too high to be applied in LTCC and τ_f value is a little large. A near-zero τ_f value was obtained by forming a solid solution with MgO or ZnO [8~9]. By adding glass frits such as H_3BO_3, Li_2O-MgO-B_2O_3 or ZnO-B_2O_3, the densification temperatures were reduced to 850~950 °C [10~12]. But the glassy phase is

detrimental to enhancing dielectric properties due to higher dielectric loss. Li_2SnO_3 has the similar rock salt structure with Li_2TiO_3 [13]. Its τ_f value was modified and $Q\times f$ values were improved by compositing with MgO, ZnO or Li_3NbO_4 [14-15]. However, the higher sintering temperatures (1200~1325 °C) and porous microstructure of Li_2SnO_3 based ceramics hindered their practical applications. Low melting fluorides (such as LiF, $CaO\text{-}B_2O_3$) were reported to be effective as sintering flux in several microwave ceramic systems [16-19].

In this work, we used MgO as an τ_f compensator and LiF as sintering aid for Li_2SnO_3 ceramics. The effects of MgO and LiF on the structural evolution, sintering characteristics, microstructures and microwave dielectric properties of Li_2SnO_3 ceramics were studied systematically.

2. Experimental procedure

Li_2SnO_3 ceramics doped with (2~13wt %) MgO and (0~6wt %) LiF were prepared by the conventional solid-state route. Li_2CO_3 (98%), SnO_2 (99.5%), MgO (99.99%) and LiF (99.6%) powders were used as starting materials. Stoichiometric Li_2CO_3 and SnO_2 were mixed according to the formula of Li_2SnO_3 and milled with ZrO_2 balls in ethanol for 8 h. Then the mixtures were dried and calcined at 700 °C for 4 h in air. The obtained Li_2SnO_3, MgO and LiF powders were weighed according to the designed molar ratios, ball-milled for 8 h, dried and sieved. Subsequently, the powders were granulated with 5wt% PVA as binder and uniaxially pressed into cylindrical disks (11.5 mm in diameter and about 6 mm in height) under a pressure of 98 MPa. These pellets were sintered at 840~1350 °C for 6 h on alumina plates at a heating rate of 4 °C/min.

The bulk densities of the sintered ceramics were measured by Archimedes method. The

crystal structures were analyzed using X-ray diffraction (XRD) with CuK_α radiation (Rigaku D/MAX2550, Tokyo, Japan). The Raman spectra were excited with the 532 nm line of a semiconductor laser at a power of 250 mW and recorded in back-scattering geometry using InVia Raman Microscope equipped with a grating filter. The microstructures were investigated using a scanning electron microscope (SEM, Quanta 200, FEI Company, Eindhoven, Holland) coupled with energy dispersive X-ray spectroscopy (EDS). The microwave dielectric properties of the specimens were measured using a network analyzer (ZVB20, Rohde & Schwarz, Munich, Germany) with the $TE_{01\delta}$ shielded cavity method. The temperature coefficient resonant frequency (τ_f) was calculated with the following formula:

$$\tau_f = \frac{(f_2 - f_1)\times 10^6}{f_1(T_2 - T_1)} \quad (1)$$

Where, f_2 and f_1 represent the resonant frequency at T_2 and T_1, respectively.

3. Results and discussion

3.1. Li_2SnO_3 doped with MgO system

Fig. 1

Fig. 1 shows the XRD patterns of (0~13)wt% MgO doped Li_2SnO_3 ceramics sintered at different temperatures. The XRD patterns displayed pure Li_2SnO_3 phase (PDF# 31-0761) for the samples doped with (0~2)wt% MgO. With increasing MgO content more than 5wt%, a novel phase of $Li_2Mg_3SnO_6$ (PDF# 39-0932) was observed accompanied by a reduction of Li_2SnO_3 phase, which is in agreement with reported [20]. This means that the following reaction occurs:

$$Li_2SnO_3 + 3MgO \rightarrow Li_2Mg_3SnO_6 \quad (2)$$

Our results are different from the reported [14], where mixtures of $Li_4MgSn_2O_7$ and Li_2SnO_3 phases were observed in Li_2SnO_3-MgO ceramics. However, our XRD results unambiguously demonstrated the existence of $Li_2Mg_3SnO_6$ indicated by the presence of $2\theta = 42.35°$ reflection peak and will be further evidenced by XRD and EDS analysis later.

Fig. 2

Table 1

The SEM images of (0~13)wt% MgO doped Li_2SnO_3 ceramics sintered at various temperatures were shown in Fig. 2. The sintered samples exhibited porous microstructure. Compared with pure Li_2SnO_3 ceramics, the MgO-doped samples displayed larger porosity, similar phenomenon were observed in Li_2TiO_3-MgO system [9]. The higher porosity of Li_2SnO_3 based ceramics was partly due to the volatilization of Li of high temperature, accompanying with weight loss up to ≥ 6wt% (Fig. 2(f)), and partly ascribed to the rapid coalescence of small subgrains which lead to the pore isolation in the large grains because of boundary breakaway [14]. The highly preferred orientation plate-like grain structures were also observed in MgO-doped samples. Table 1 present bulk densities and microwave dielectric properties of MgO-doped Li_2SnO_3 ceramics sintered at optimum temperatures. With increasing MgO content, bulk density and dielectric permittivity decreased due to lighter weight and lower ε_r value (9.7) of MgO. It is noteworthy that MgO addition improved $Q \times f$ and frequency-temperature stability. Well dielectric properties of $\varepsilon_r \sim 13.2$, $Q \times f \sim 57000$ GHz, and $\tau_f = -0.0$ ppm/°C was obtained at 1325 °C for Li_2SnO_3-8wt% MgO (LSM) ceramics.

3.2. Li_2SnO_3-8 wt% MgO doped with LiF system

Fig. 3

Table 2

In order to decrease the sintering temperature lower than 950 °C for LTCC applications, LiF powders were added into LSM matrix. Fig. 3 illustrates the XRD patterns of *x*wt% ($0 \leq x \leq 6$) LiF doped LSM ceramics sintered at different temperatures. The XRD patterns exhibited a two-phase system with a monoclinic Li_2SnO_3 and a cubic $Li_2Mg_3SnO_6$ phase. The amount of $Li_2Mg_3SnO_6$ phase increased with increasing LiF content (x). Furthermore, the peaks of $2\theta = 18°$ shifted toward higher angle then back toward lower ones with increasing LiF content, which implied lattice contraction and lattice expansion. Table 2 displays the variation in lattice constant of Li_2SnO_3 ceramics with increasing LiF content. The lattice contraction might be owing to the substitution of the F^- ion (R = 1.33 Å) in the O^{2-} (R = 1.4 Å) sites, the similar phenomenon was observed in Li_2TiO_3-LiF system [16]. The replacement mechanisms as following:

$$3LiF \xrightarrow{Li_2SnO_3} Li'''_{Sn} + 3F^{\bullet}_{O} + 2Li^{\times}_{Li} \quad (3)$$

While LiF addition $x \geq 6$wt%, the increase of lattice constant was associated with a large extent of liquid phase during sintering process inhibit the entrance or occupation of Li^+ and F^- in the Li_2SnO_3 lattice.

Fig. 4

The Raman spectra of LSM-*x*wt% LiF ceramics sintered at different temperatures are given in Fig. 4. The spectra of $x \geq 1$ samples were similar to that of pure LSM, which exhibited several first order Raman active modes at 242 cm^{-1}, 369 cm^{-1} and 591 cm^{-1}. The width of the mode increased with increasing x implying that the arrangement of atoms in crystal became more disorderly, in agreement with the reported [21~22]. A new broad band near 650 cm^{-1}, which was considered to associate with $Li_2Mg_3SnO_6$ phase (its Raman spectra is given in insert of Fig. 4), was observed with increasing LiF content.

Fig. 5

Addition of LiF as sintering aid in the LSM ceramics can bring about two effects during the sintering process. On one hand, liquid phase can be formed during the sintering because of lower melting point of LiF (845 °C), which could enhance grain boundary mass transport significantly. On the other hand, the substitution of smaller F^- for O^{2-} would cause weakening of oxygen bond strength which reduces the intrinsic sintering temperature and facilitates the diffusion process [22]. The SEM images of LSM-*x*wt% LiF ($1 \leq x \leq 6$) ceramics sintered at 880 °C are shown in Fig.5. It can be seen that all specimens demonstrated well-dense microstructure, indicating LiF doping effectively promoted grain growth and improved densification. The coexistence of Li_2SnO_3 and $Li_2Mg_3SnO_6$ in specimens can be observed by distinguishing from their EDS analysis. As shown in Fig. 5(e) and (f), the grain A showed much lower content of Mg compared with the grain B.

Fig. 6

Fig. 6 summarizes the bulk density and weight loss of LSM-*x*wt% LiF ($1 \leq x \leq 6$) ceramics as functions of sintering temperatures and LiF content. With increasing *x*, bulk densities increased and then decreased after reaching their respective maximum values. For LiF-added LSM ceramics, the weight loss was reduced from 6.0wt% to 2.2wt%. The densification temperatures tended to shift down from 900 °C to 860 °C as increasing *x* from 1 to 6. Typically, LSM-2wt% LiF sample sintered at 880 °C achieved a maximum density of 4.64 g/cm^3, which is equivalent to a relative density of 97.5 %. This further confirmed the effectiveness of LiF in improving sinterability of LSM ceramics due to liquid-phase sintering and inhibition of Li volatile. Furthermore, when $x > 2$, the densities decreased because of lower theoretical density of $Li_2Mg_3SnO_6$ (3.27 g/cm^3) than that of Li_2SnO_3 (4.96 g/cm^3).

Fig. 7

The variation of microwave dielectric properties of LSM-*x*wt% LiF ($1 \leq x \leq 6$) ceramics with increasing sintering temperatures and LiF content were demonstrated in Fig. 7(a~c). As shown in Fig. 7(a) and (b), the variations in ε_r and $Q \times f$ values with sintering temperatures and *x* were consistent with that of bulk density, suggests that the density is the dominating factor to control ε_r and $Q \times f$ values in Li_2SnO_3-MgO-LiF ceramics. According to the Clausius-Mossotti equation, the dielectric constant of ceramic material is predominantly decided by the dipoles in unit cell volume and dielectric polarizabilities of ions [23]. To be

specific, higher density exhibits higher ε_r value as a result of more dipoles and more apt to be polarized. It is well known that the dielectric loss is mainly caused not only by the lattice vibrational modes, but also by impurities, second phase, pores, lattice defect, grain boundary and grain morphology [24-25]. Thus, LiF doping effectively improved ε_r and $Q\times f$ values as a result of well-dense microstructures and higher density. In addition, with increasing LiF content, the decrease in ε_r values was in connection with the comparative lower dielectric polarizabilities of F^- (1.62 $Å^3$) than that of O^{2-} (2.01 $Å^3$). And the increase of $Q\times f$ values is attributed to increasing content of $Li_2Mg_3SnO_6$ ($Q\times f$ = 123000 GHz, τ_f = -32 ppm/°C) [26] and uniform microstructures. It can be seen in Fig. 7(c), the τ_f value showed a continuous negative increase in magnitude as increasing LiF content owing to negative τ_f value of $Li_2Mg_3SnO_6$. In general, τ_f is well known to be influenced by the composition, the additive and the second phase of the materials [27]. Through appropriate adjustment, excellent microwave dielectric properties of ε_r = 14.7, $Q\times f$ = 78400 GHz and τ_f = -0.9 ppm/°C were obtained at 880 °C for LSM-2wt% LiF ceramics.

Fig. 8

Fig. 8 presents the XRD pattern and SEM image of the LSM-2wt% LiF ceramics doped with 10wt% silver (Ag) powders sintered at 880 °C for 2 h. As shown in Fig. 8, multiphase of Li_2SnO_3, $Li_2Mg_3SnO_6$ and respective metals (Ag) were observed. No additional peaks in the XRD patterns were detected, implying that no chemical reaction had taken place among LSM-2wt% LiF ceramics and Ag powders. Thus, LiF-doped LSM ceramics were suitable

candidates for LTCC applications because of their lower sintering temperatures, excellent microwave dielectric properties and compatibility with Ag electrode.

4. Conclusions

Li_2SnO_3 ceramics co-doped with MgO and LiF were prepared by a conventional solid-state method. With increasing MgO content, a novel phase $Li_2Mg_3SnO_6$ was observed accompanied by a reduction of Li_2SnO_3. The frequency-temperature stability of Li_2SnO_3 ceramics was improved by MgO doping. Good microwave dielectric properties of ε_r = 11, $Q \times f$ = 57000GHz, and τ_f = -0.0 ppm/°C were obtained at 1325 °C for Li_2SnO_3-8wt% MgO ceramics. LiF addition significantly promoted the sinterability of LSM ceramics and successfully reduced the sintering temperatures to below 900 °C. Furthermore, LiF addition not only inhibited volatile of Li but also promoted synthesis of $Li_2Mg_3SnO_6$. The microwave dielectric properties of LSM ceramics were further optimized due to increasing $Li_2Mg_3SnO_6$ content. LSM-2wt% LiF ceramics exhibited well-densified structures and excellent microwave dielectric properties of ε_r = 14.7, $Q \times f$ = 78400 GHz, and τ_f = -0.9 ppm/°C at 880 °C. Good compatibility existed between the LSM-2wt% LiF matrix and Ag powders, making them suitable for LTCC applications.

Acknowledgments

This work is supported by the National Natural Science Foundation of China (Grant nos. 51272150, 51572162 and 51132003), the Scientific Research Foundation of Shaanxi Normal University (Grant no. X2013YB01), Specialized Research Fund for the Doctoral Program of Higher Education (No. 20120202110004) and the Fundamental Research Funds for the Central Universities (GK201401003).

References

[1] M. Hagymási, A. Roosen, R. Karmazin, O. Devnovsek, W. Haas, Constrained sintering of dielectric and ferrite LTCC tape composites, J. Eur. Ceram. Soc. 25 (2005) 2061-2064.

[2] L. Cheng, P. Liu, X.M. Chen, et al., Fabriction of nanopowders by high energy ball milling and low temperature sintering of Mg_2SiO_4 microwave dielectrics, J. Alloy. Compds. 513 (2012) 373-377.

[3] G.G. Yao, P. Liu, H.W. Zhang, Novel series of low-firing microwave dielectric ceramics: $Ca_5A_4(VO_4)_6$ (A^{2+}= Mg, Zn), J. Am. Ceram. Soc. 96 (2013) 1691-1693.

[4] G.G. Yao, P. Liu, H.W. Zhang, Low-temperature sintering and microwave dielectric properties of $(Mg_{0.95}Zn_{0.05})_2(Ti_{0.8}Sn_{0.2})O_4$-$(Ca_{0.8}Sr_{0.2})TiO_3$ composite ceramics, J. Am. Ceram. Soc. 96 (2013) 3114-3119.

[5] L.X. Pang, D. Zhou, Microwave dielectric properties of low-firing Li_2MO_3 (M = Ti, Zr, Sn) ceramics with B_2O_3-CuO addition, J. Am. Ceram. Soc. 93 (2010) 3614-3617.

[6] L.X. Pang, H. Liu, D. Zhou, et al., Low-temperature sintering and microwave dielectric properties of Li_3MO_4 (M = Ta, Sb) ceramics, J. Alloys. Compds. 525 (2012) 22-24.

[7] S. George, M.T. Sebastian, Synthesis and microwave dielectric properties of novel temperature stable high Q, $Li_2ATi_3O_8$ (A = Mg, Zn) ceramics, J. Am. Ceram. Soc. 93 (2010) 2164-2166.

[8] J. J. Bian, Y.F. Dong, New high Q microwave dielectric ceramics with rock salt structures: $(1-x)Li_2TiO_3 + xMgO$ system ($0 \leq x \leq 0.5$), J. Eur. Ceram. Soc. 30 (2010) 325-330.

[9] C.L. Huang, Y.W. Tseng, J.Y. Chen, High-Q dielectric using ZnO-modified Li_2TiO_3 ceramics for microwave applications, J. Eurp. Ceram. Soc. 32 (2012) 3287-3295.

[10] J. Liang, W.Z. Lu, J.M. Wu, et al., Microwave dielectric properties of Li_2TiO_3 ceramics sintered at low temperatures, Mater. Sci. Eng. B, 176 (2011) 99-102.

[11] G.H. Chen, M.Z. Hou, Y. Yang, Microwave dielectric properties of Low-fired Li_2TiO_3 ceramics doped with Li_2O-MgO-B_2O_3 frit, Mater. Lett. 89 (2012) 16-18.

[12] J. Liang, W.Z. Lu, Microwave dielectric properties of Li_2TiO_3 ceramics doped with ZnO-B_2O_3 frit, J. Am. Ceram. Soc. 92 (2009) 952-954.

[13] J.L. Hodeau, M. Marezio, Neutron profile refinement of the structures of Li_2SnO_3 and Li_2ZrO_3, J. Solid State Chem. 45 (1982) 170-179.

[14] C.W. Liu, N.X. Wu, Y.L. Mao, J.J. Bian, Phase formation, microstructure and microwave dielectric properties of Li_2SnO_3-*M*O (*M* = Mg, Zn) ceramics, J. Electroceram. 32 (2014) 199-204.

[15] N.X. Wu, J.J. Bian, Microstructure and microwave dielectric properties of (1-*y*)Li_3NbO_4 + *y*Li_2TiO_3(Li_2SnO_3) ceramics, Mater. Sci. Eng. B, 177 (2012) 1793-1798.

[16] Y.Z. Hao, H. Yang, G.H. Chen, Q.L. Zhang, Microwave dielectric properties of Li_2TiO_3 ceramics doped with LiF for LTCC applications, J. Alloys. Compds. 552 (2013) 173-179.

[17] N.X. Xu, J.H. Zhou, H. Yang, Structural evolution and microwave dielectric properties of MgO-LiF co-doped Li_2TiO_3 ceramics for LTCC applications, Ceram. Int. 40 (2014) 15191-15198.

[18] U. Intatha, S. Eitssayeam, K. Pengpat, K.J.D. Mackenzie, T. Tunkasiri, Dielectric properties of low temperature sintered LiF doped $BaFe_{0.5}Nb_{0.5}O_3$, Mater. Lett. 61 (2007) 196-200.

[19] S.H. Lei, H.Q. Fan, W.N. Chen, Effects of CaO-B_2O_3 glass addition on the

low-temperature sintering and cation ordering in $SrxLa_{(1-x)}TixAl_{(1-x)}O_3$ ceramics. J. Alloy. Compd., 632 (2015) 78-86.

[20] A.N.J. Keulen, G.C. Hoogendam, K. Seshan, J.G. van Ommen, J.R.H. Ross, The role of Tin in Li/Sn/MgO catalysts for the oxidative coupling of methane, J. Chem. Soc., Chem. Commun. (1992) 1546-1547.

[21] Y.M. Ding, J.J. Bian, Structural evolution, sintering behavior and microwave dielectric properties of $(1-x)Li_2TiO_3+xLiF$ ceramics, Mater. Res. Bull. 48 (2013) 2776-2781.

[22] W.N. Chen, H.Q. Fan, C.B. Long, et al. Effects of sintering time on crystal structure, dielectric properties and conductivity of $(Ca_{0.8}Sr_{0.2})ZrO_3$ ceramics. J. Mater. Sci: Mater. Electron., 25(2014) 1505-1511.

[23] M.T. Sebastian, Dielectric materials for wireless communication, Elsevier, 2010.

[24] H. Tamura, Microwave dielectric losses caused by lattice defects, J. Eur. Ceram. Soc. 26 (2006) 1775-1780.

[25] B.D. Silverman, Microwave absorption in cubic strontium titanate, Phys. Rev. 125 (1962) 1921-1930.

[26] Z.F. Fu, P. Liu, J.L. Ma, et al., Novel series of ultra-low loss microwave dielectric ceramics: $Li_2Mg_3BO_6$ (B= Ti, Sn, Zr), J. Europ. Ceram. Soc., 36 (2016) 625-629.

[27] C.L. Huang, J.Y. Chen, Low-Loss Microwave Dielectric Ceramics Using $(Mg_{1-x}Mn_x)_2TiO_4$ (x= 0.02–0.1) Solid Solution, J. Am. Ceram. Soc. 92 (2009) 675-678.

Figure captions

Fig. 1. XRD patterns of Li_2SnO_3 ceramics doped with (0~13) wt% MgO.

Fig. 2. (a~e) SEM images of Li_2SnO_3 ceramics doped with (0~13) wt% MgO and (f) weight loss of ceramics.

Fig. 3. XRD patterns of LSM-*x* wt% LiF ceramics sintered at different temperatures.

Fig. 4. Raman spectra of LSM-*x* wt% LiF ceramics sintered at different temperatures. Inset is the Raman spectra of $Li_2Mg_3SnO_6$.

Fig. 5. (a~d) SEM images of LSM-*x* wt% LiF ceramics and (e~f) the EDS datum of grain A and B.

Fig. 6. The bulk density and weight loss of LSM-*x* wt% LiF ceramics sintered at different temperatures.

Fig. 7. Variation of microwave dielectric properties of LSM-*x* wt% LiF ceramics sintered at various temperatures with different LiF contents.

Fig. 8. The XRD pattern and SEM image of the LSM-2 wt% LiF ceramics doped with 10 wt% Ag powder sintered at 880 °C for 2 h.

Figure 1

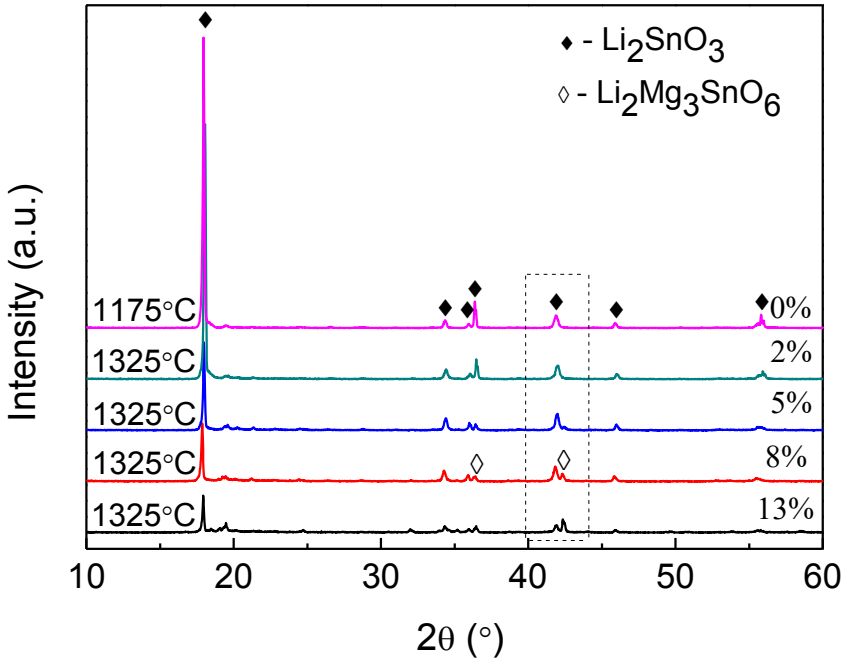

Figure 2

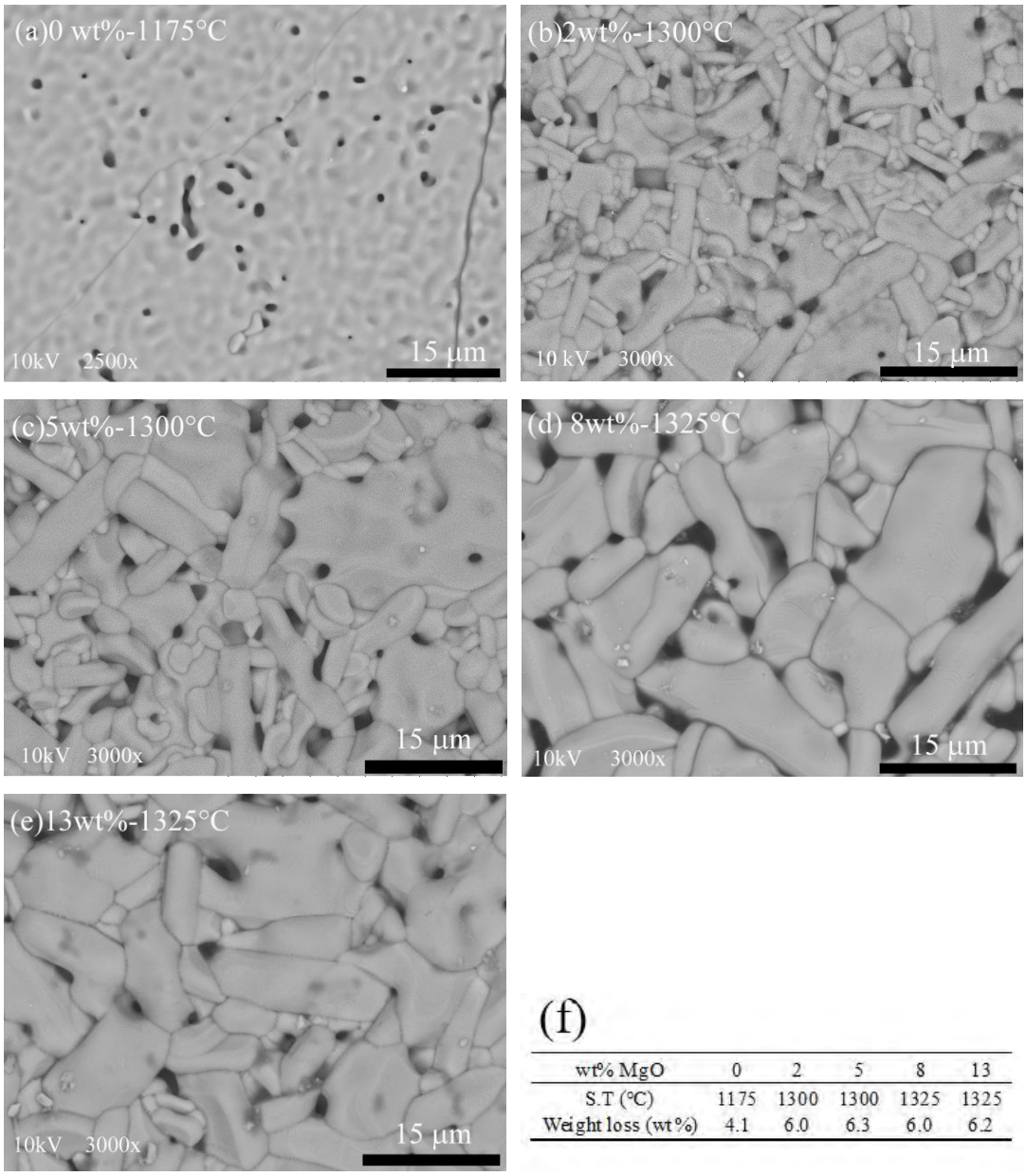

(f)

wt% MgO	0	2	5	8	13
S.T (℃)	1175	1300	1300	1325	1325
Weight loss (wt%)	4.1	6.0	6.3	6.0	6.2

Figure 3

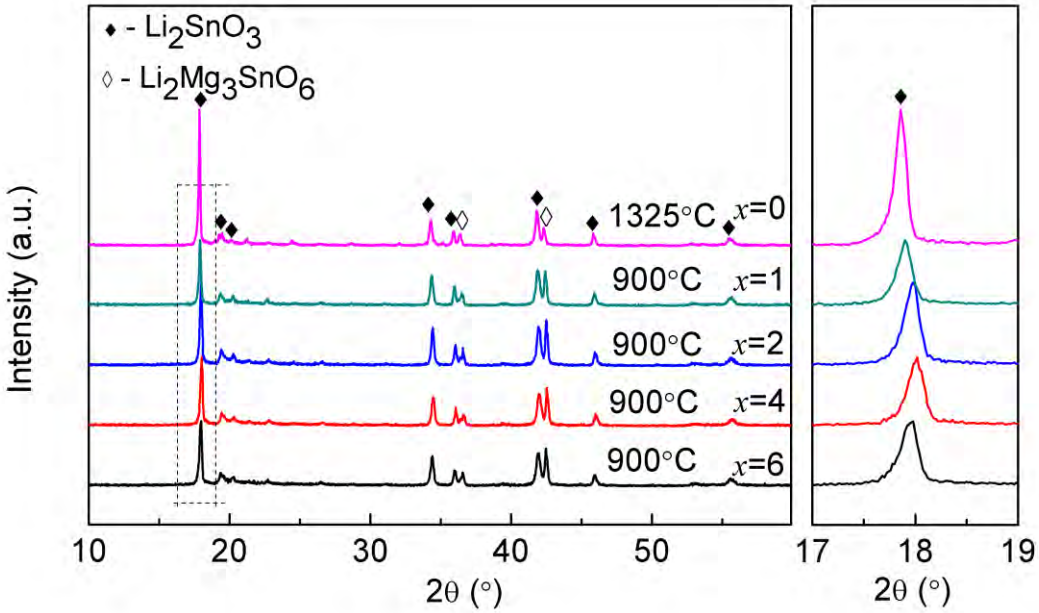

Figure 4

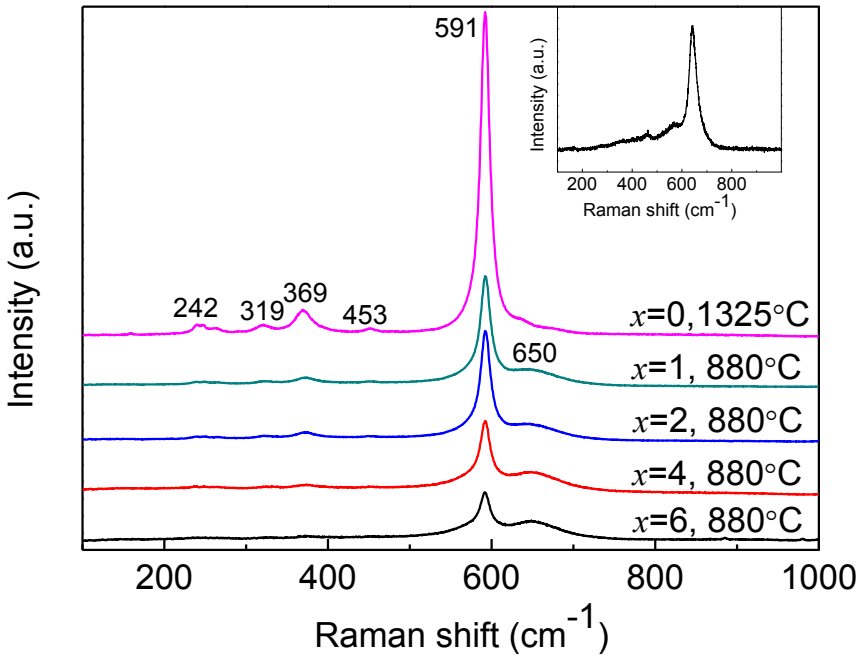

Figure 5

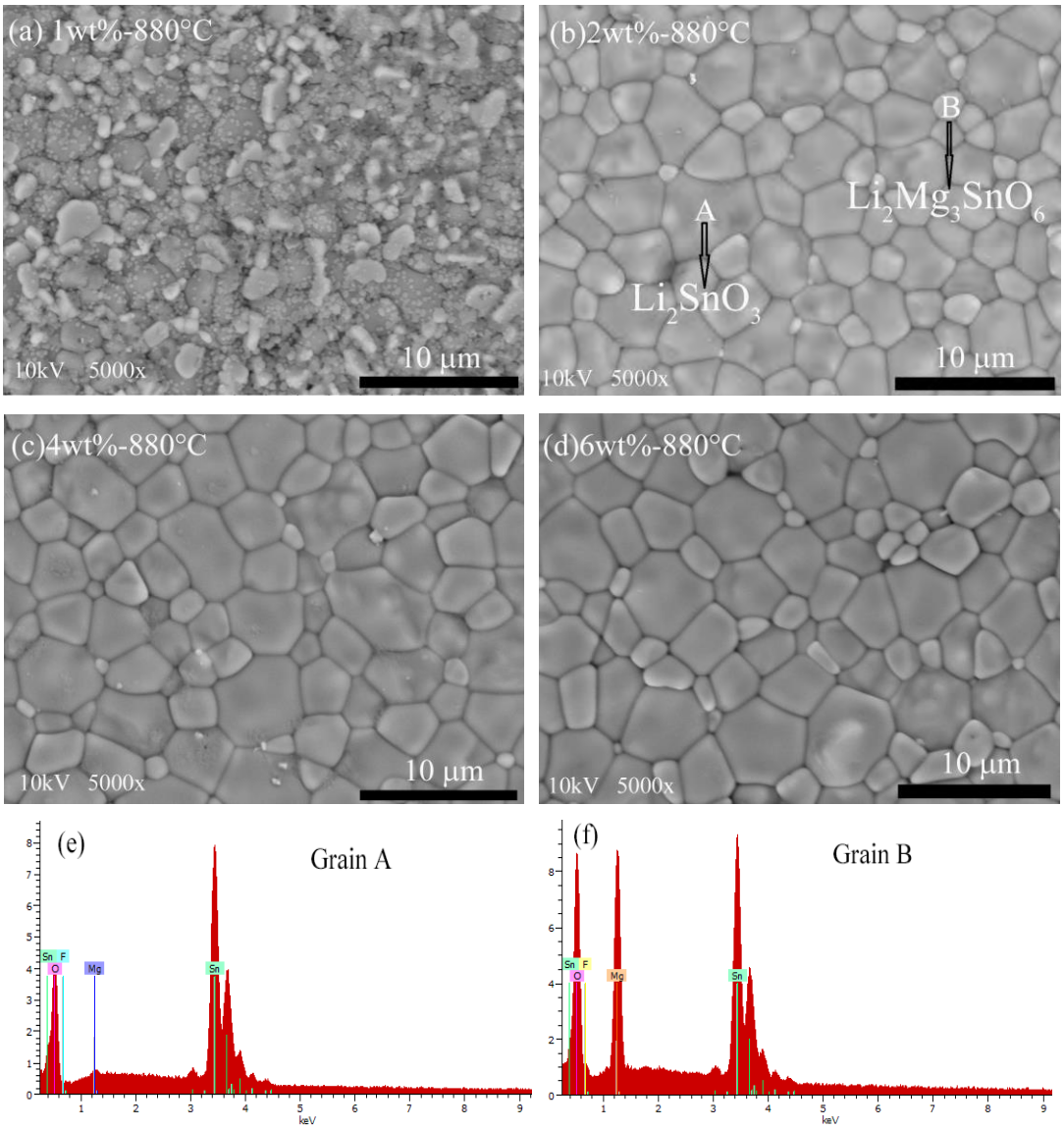

Figure 6

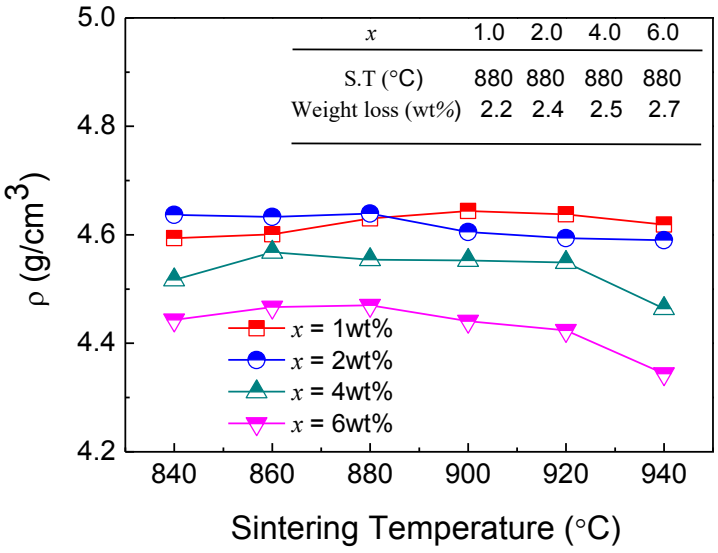

Figure 7

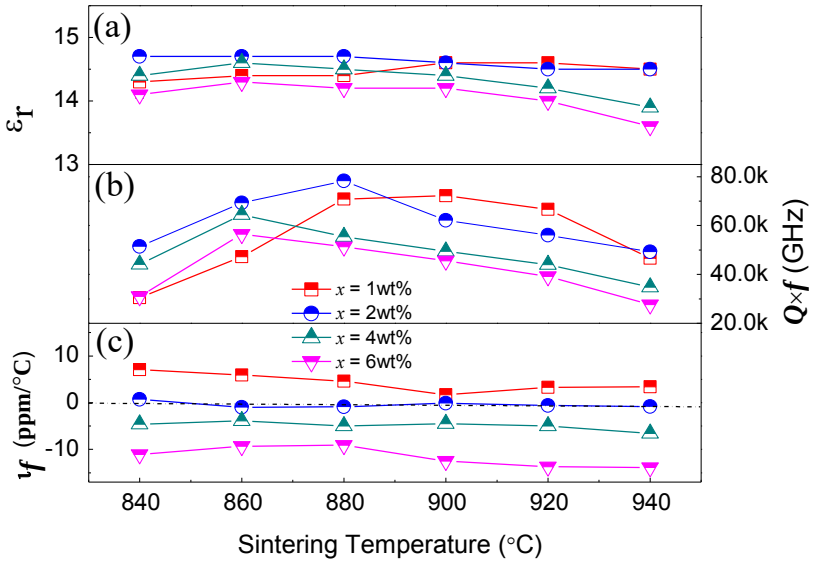

Figure 8

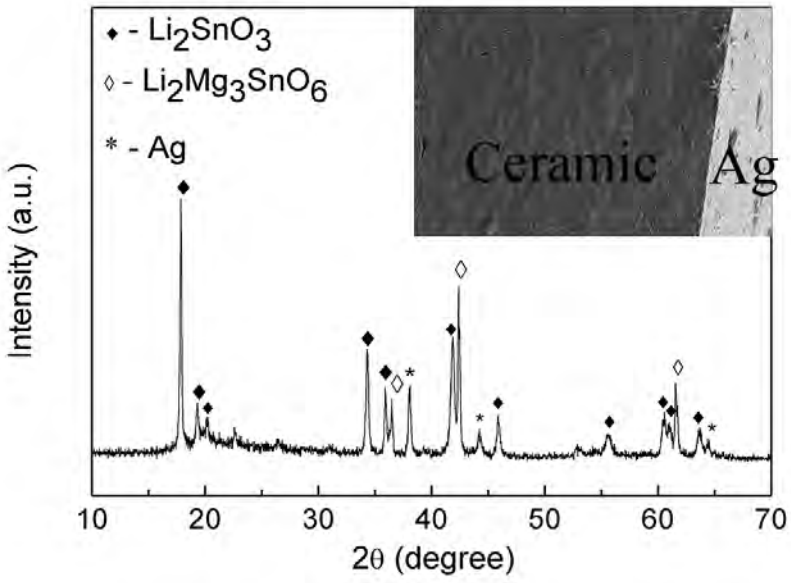

Table 1 The density and microwave dielectric properties of Li_2SnO_3 ceramics doped with (0~13) wt% MgO and sintered at optimum temperatures.

wt% MgO	S.T (°C)	ρ (g/cm^3)	ε_r	tan δ	$Q\times f$ (GHz)	τ_f (ppm/°C)
0	1175	4.86	14.7	0.00024	36900	+24.8
2	1300	4.39	13.4	0.00022	43700	+17.6
5	1300	4.39	13.2	0.00017	52500	+13.0
8	1325	4.29	13.2	0.00016	57000	+0.0
13	1325	4.28	12.7	0.00020	48400	-8.0

Table 2 The lattice constant of Li_2SnO_3 ceramics with different LiF content.

x	S.T (°C)	a (Å)	b (Å)	c (Å)	V (Å^3)	β (°)
0	1325	5.3163	9.1881	10.0673	483.77	100.34
1	900	5.3032	9.1745	10.0589	481.67	100.21
2	900	5.2721	9.1605	9.9602	474.27	99.61
4	900	5.2670	9.1502	9.9499	472.84	99.59
6	900	5.2857	9.1631	10.0128	477.69	99.93